Assessment of Thermal Fatigue for Helical Steam Generator during Density Wave Oscillations with MARS-KS

Jun Ha Hwang [a], Jeong Ik Lee [a*]
[a]*Department of Nuclear and Quantum Engineering, Korea Advanced Institute of Science and Technology, 373-1 Guseong-dong Yuseong-gu, Daejeon 305-701, Republic of Korea*
[*]*Corresponding author: jeongiklee@kaist.ac.kr*

Keywords : Helical Tube, MARS-KS, Density Wave Oscillation, Two-phase Instability, Thermal fatigue

1. Introduction

Nuclear energy is increasingly recognized as a vital solution for deep decarbonization and stable baseload power. In this context, Small Modular Reactors (SMRs) like Korea's SMART and China's HTR-PM have gained significant attention due to their enhanced safety and modular flexibility [1]. These reactors often employ Helical Steam Generators (HSGs) with a once-through configuration. However, the once-through design, combined with parallel channel configurations, makes HSGs inherently susceptible to Density Wave Oscillations (DWO), which can lead to cyclic thermal stresses and subsequent thermal fatigue on the tube walls [2].

To ensure the structural integrity of steam generators, system-level thermal-hydraulic codes such as MARS-KS are employed to evaluate the impact of DWO. However, it has been observed that 1D system codes often yield significantly different results compared to experimental data due to the simplified modeling of two-phase flow dynamics in complex geometries like helical tubes. Specifically, current numerical models tend to over-predict the amplitude and the frequency of oscillations, leading to an excessively conservative estimation of thermal stress variation. While such conservatism is generally preferred in safety analysis, excessive over-prediction can lead to overly restrictive operational constraints.

Therefore, it is necessary to quantify the degree of conservatism in MARS-KS by comparing its predictions with experimental data. By performing a Verification and Validation (V&V) focused on wall temperature oscillation characteristics, the discrepancy between numerical results and experimental data can be established as a "Correction Ratio." This approach allows for a more realistic assessment of the thermal-hydraulic behavior and structural health of full-scale steam generators.

In this study, the V&V of MARS-KS is conducted using experimental data obtained from a helical tube test facility. The study focuses on quantifying the conservative bias of the code in terms of oscillation amplitude and frequency. Based on these findings, a calibrated evaluation of thermal fatigue is performed for advanced reactors, including SMART and HTR-PM. By applying the derived correction factors to the MARS-KS results under actual reactor conditions, this research aims to provide a more accurate yet safety-ensured technical basis for the long-term reliability of next-generation helical steam generators.

2. Experimental Setup

2.1 Helical Tube DWO Test Facility

As shown in figure 1, the dedicated experimental loop was employed to investigate Density Wave Oscillation (DWO) in helical coil steam generators. This facility, upgraded from the setup by Oh et al. (2025), features three asymmetric helical tubes with varying curvatures and lengths to capture geometric effects on flow stability [3]. The closed-loop system includes a circulation pump, a pre-heater for inlet subcooling control, and a multi-electrode DC heating system for heating helical tubes. The features of the helical tube geometry and measurement uncertainty are listed in Tables 1 and 2.

Fig. 1. Helical Tube DWO Test Facility.

Table I: Measurement uncertainty

Instrument	Uncertainty
Coriolis flowmeter	0.02 %
Vortex flowmeter	2.00 %
K-type thermocouple	0.53 °C
Pressure transmitter	0.36 kPa

Table II: Helical Tube Geometry

	Experimental facility		
I.D 6 mm	Tube 1	Tube 2	Tube 3
Helix angle (°)	8.52	8.16	7.59
Helical diameter (mm)	288.50	468.50	648.50
Tube pitch (mm)	135.71	211.11	271.43
Tube length (m)	12.83	13.38	14.39
Tube turns	14.00	9.00	7.00

2.2 Wall Temperature Measurement

To evaluate the thermal-hydraulic transients during DWO, wall temperatures were monitored at the inlet, mid-point (1/2 length), and outlet of each helical tube as shown in figure 2. K-type thermocouples were utilized, secured to the outer surface of the SUS316 tubes with Kapton tape. To minimize external heat loss and approximate adiabatic conditions, the test sections were shielded with multi-layered ceramic wool insulation.

Due to the complex helical geometry, the measured outer surface temperatures were subject to a systematic bias, typically recording lower than actual wall temperatures due to thermal resistance at the junction and heat losses via lead-wire conduction and radiation. To resolve this, a correction method based on a thermal resistance network and quasi-steady energy balance was implemented to determine the actual surface temperature. For structural integrity analysis, the first helical tube was selected as the representative point, as it experiences the most significant heat load and temperature fluctuations. The measurement system demonstrated high consistency between the periods of flow rate and wall temperature oscillations, confirming its capability to capture transient thermal phenomena.

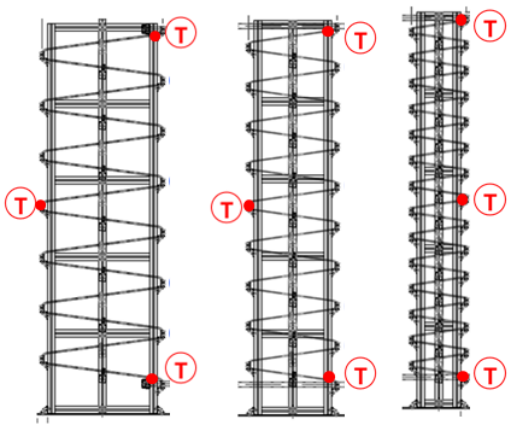

Fig. 2. Locations of wall thermocouples at inlet, center, and outlet.

2.3 Simulant Fluid and Flow Scaling

Novec-649 was selected as the working fluid to simulate the low liquid-to-vapor density ratios (ρ_l/ρ_g) of advanced reactors at laboratory-scale pressures below 10 bar. This refrigerant provides a safe and economical alternative to high-pressure water experiments while ensuring minimized global warming potential. To maintain macro-scale flow characteristics where gravity and inertia dominate, the Confinement number (Co), as shown in equation 1, was verified for the 6 mm diameter tubes.

$$Co = \frac{1}{D_h}\sqrt{\frac{\sigma}{g(\rho_l - \rho_g)}} \quad (1)$$

The Co number for Novec-649 remained below 0.13 across all operating conditions, placing it reliably within the macro-scale regime (Co < 0.3). This validation confirms that the experimental facility effectively minimizes surface tension effects, providing a physically consistent simulation of the flow dynamics in actual reactor steam generator tubes.

2.4 Experimental Conditions for DWO Evaluation

To evaluate the thermal fatigue induced by DWO, three specific cases were selected where sustained oscillations were clearly observed. These cases represent different outlet pressure levels (3.4 to 5.2 bar) with corresponding mass fluxes and heating powers, as summarized in Table III. These boundary conditions were utilized as the benchmark for MARS-KS validation to quantify the code's conservatism in predicting oscillation characteristics under unstable flow regimes.

Table III: Problem Description

Case	1	2	3
Mass flux (kg/m^2s)	430	540	590
Inlet temperature (℃)	50	52	48
Outlet pressure (bar)	3.4	4.4	5.2
1st Tube Heating Power (W)	1740	2370	3560

3. Numerical Methodology

3.1 Code Implementation and Reference Model

The accurate prediction of Density Wave Oscillation (DWO) in helical tubes is fundamentally dependent on the precision of the frictional pressure drop calculation, as DWO is a dynamic instability driven by the feedback between flow inertia and system pressure drop. However, the standard version of MARS-KS 2.0 is primarily optimized for straight pipe geometries and lacks dedicated models to account for the complex flow dynamics inherent in helical configurations. In a helical flow path, centrifugal forces induce secondary flow patterns (Dean flow) that significantly alter the friction factor and phase distribution compared to straight tubes.

To overcome these geometric limitations, this study utilized a modified version of MARS-KS that integrates specialized helical correlations into its source code,

following the methodology established by Oh et al. (2024) [4]. For single-phase flow, the Ito correlation was implemented to determine the friction factor f in equation 2, incorporating the interaction between the Reynolds number and the curvature ratio (d/D) to reflect the increased resistance caused by secondary flows [5].

$$f\left(\frac{D}{d}\right)^{\frac{1}{2}} = 0.029 + 0.304\left[Re\left(\frac{d}{D}\right)^{2}\right]^{-0.25} \quad (2)$$

For two-phase conditions, the Colombo correlation was adopted to calculate the two-phase frictional multiplier Φ_l^2 [6]. This model is specifically designed for helical geometries, as it accounts for the centrifugal effects on phase distribution through a modified Lockhart-Martinelli parameter X_{tt} as shown in equation 3.

$$\Phi_{\mathrm{l}}^2 = 0.0986\left(1 + \frac{20}{x_{tt}} + \frac{1}{X_{tt}^2}\right) De_l^{0.19}\left(\frac{\rho_m}{\rho_l}\right)^{-0.4}$$
$$\mathrm{De_l} = \frac{G(1-x)d}{\mu_l}\sqrt{d/D}, \qquad \rho_m = \left(\frac{x}{\rho_g} + \frac{1-x}{\rho_f}\right)^{-1} \quad (3)$$

By enhancing the pressure drop modeling for helical geometries, the code's ability to capture the feedback loops driving DWO was significantly improved regardless of the working fluid. This refinement ensures that the numerical model provides a physically sound representation of the internal flow dynamics in helical steam generators (HSGs), establishing a robust technical basis for evaluating both experimental results and reactor-scale performance.

3.2 Nodalization and Component Configuration

The numerical model was constructed using the modified MARS-KS code to capture the transient thermal-hydraulic behavior of helical steam generators. The nodalization scheme incorporates several standard MARS-KS components to define the flow paths and boundary conditions accurately as shown in figure 3. Specifically, 'Time Dependent Volume' (TMDPVOL) and 'Single Volume' components are utilized to establish the inlet flow conditions and outlet pressure boundaries. These volumes are connected to 'Branch' components that function as the inlet and outlet headers for flow distribution and recombination. The helical tubes themselves are represented by 'PIPE' components, where each pipe is divided into multiple volumes (nodes) to track the axial progression of phase change and wall temperature variations. Heat structures are coupled with these 'PIPE' components to apply uniform heat flux profiles.

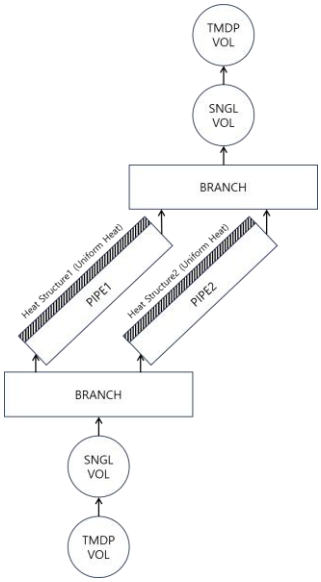

Fig. 3. Nodalization of Uniform Heating Helical Tube

3.3 Geometric Modeling Strategy for Validation and Evaluation

The modeling approach for the helical geometry was bifurcated to distinguish between the validation of experimental data and the assessment of full-scale advanced reactors. For the validation phase, the nodalization was designed to strictly reflect the actual physical dimensions of the three asymmetric helical tubes used in the test facility. This rigorous modeling ensures that the code's predictions for oscillation periods and amplitudes are compared against the exact geometric constraints of the experimental loop.

In contrast, when evaluating the structural integrity of advanced Small Modular Reactors (SMRs) such as SMART and HTR-PM, a simplified modeling strategy was adopted for computational efficiency. Instead of replicating the hundreds of tubes found in a commercial steam generator, the system was simplified into a two-parallel-pipe model.

4. Result and Discussions

4.1 Comparative Assessment of DWO Characteristics and Development of Calibration Framework

The transient thermal-hydraulic response during Density Wave Oscillation (DWO) was evaluated by comparing experimental measurements from the test facility with numerical predictions from the modified MARS-KS code. Experimental observations, illustrated in figures 4 through 6, demonstrated a high degree of synchronization between the oscillation periods of the inlet flow rate and the wall temperatures at the inlet and outlet. In the flow rate plots, the shaded gray region visualizes the statistical range defined by the mean $\pm$ the 95th percentile amplitude (Amp95). This region encompasses approximately 95% of the oscillation data, serving as a robust metric that filters out transient experimental noise and numerical outliers to provide a

representative oscillation magnitude. This high synchronization at the inlet and outlet is interpreted as a result of direct convective coupling, where heat transfer variations induced by flow instability are immediately transferred to the tube wall.

However, local discrepancies in the oscillation period were observed at the center, which can be attributed to its position within the two-phase flow regime influenced by upstream oscillations and inherent thermal-hydraulic inertia. While the boiling boundary primarily oscillates at a location upstream of the center, this movement induces periodic fluctuations in the local quality and void fraction as the flow passes through the mid-point. This downstream propagation of quality waves, combined with the thermal-hydraulic inertia of the fluid and the tube wall, is postulated to create a non-linear phase-shift and significant thermal lag. This inertia, acting as a damping mechanism, potentially distorts the temperature response relative to the inlet flow, causing the observed deviations in the dominant oscillation period. Furthermore, the irregular behavior of the liquid film inherent in the two-phase region may further disturb the macro-scale periodicity.

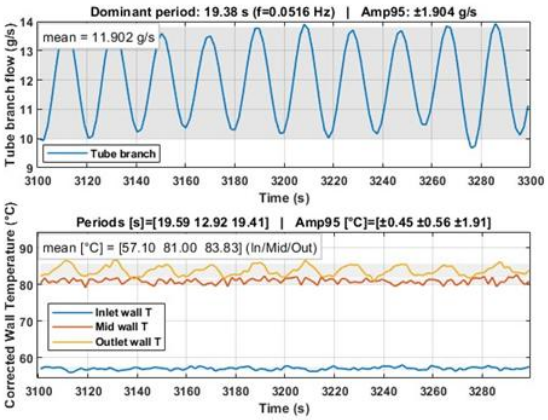

Fig. 4. Flow and Thermal Oscillations due to DWO (Case 1)

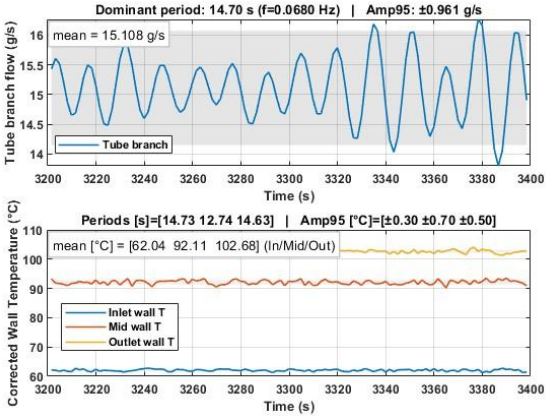

Fig. 5. Flow and Thermal Oscillations due to DWO (Case 2)

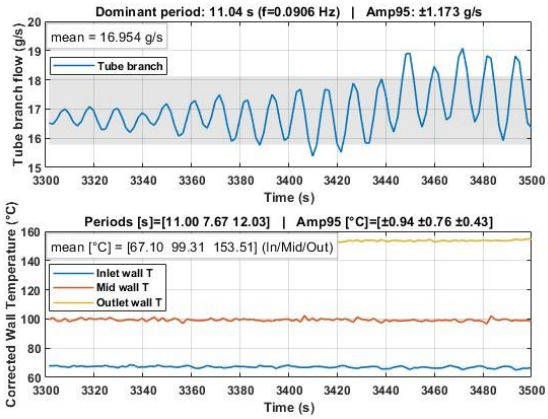

Fig. 6. Flow and Thermal Oscillations due to DWO (Case 3)

Quantitatively, MARS-KS captured the physical trend of decreasing oscillation periods with increasing pressure but exhibited significant numerical conservatism. As summarized in Tables IV and V, the code consistently over-predicted the wall temperature oscillation amplitude (Amp95) and under-predicted the period. These discrepancies may be attributed to the inherent characteristics of the constitutive models in MARS-KS, which were primarily developed and validated using water as the reference fluid. The application of these correlations to Novec-649—characterized by a significantly higher vapor density compared to water—potentially introduces a systematic bias in the calculation of acceleration losses. Such a mismatch is consistent with the observed over-prediction of local pressure drops, which leads to artificial shifts in saturation temperature boundaries and the resulting numerical conservatism in wall temperature amplitudes.

Table IV: MARS-KS predicted wall temperature amplitudes relative to experimental data

Case	Inlet	Center	Outlet
1 (3.4 bar)	817.1%	337.9%	4.1%
2 (4.4 bar)	1201.7%	223.3%	94.6%
3 (5.2 bar)	275.7%	252.2%	184.4%

Table V: MARS-KS predicted wall temperature Period relative to experimental data

Case (P_{out})	Inlet	Center	Outlet
1 (3.4 bar)	-47.7%	-21.1%	-47.5%
2 (4.4 bar)	-42.4%	-33.4%	-40.7%
3 (5.2 bar)	-44.1%	-19.8%	-48.9%

To provide a clear physical basis for these axial discrepancies, the temperature-dependent electrical resistivity of the SS316 tube was analyzed. As demonstrated in Figure 7, the electrical resistivity of SS316 increases linearly with temperature. Under the DC heating conditions used in this experiment, where the current remains constant along the tube, this property results in a non-uniform axial heat power distribution. The local heating power rises toward the outlet ($P/P_{avg} \approx 1.05$) and remains lower at the inlet ($P/$

$P_{avg} \approx 0.93$), creating a systematic bias compared to the uniform heat flux assumed in the numerical model.

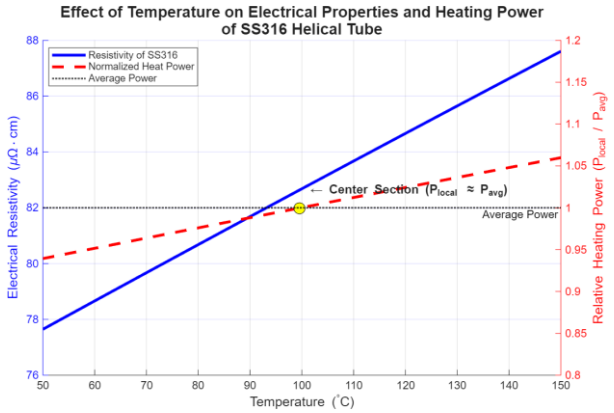

Fig. 7. Temperature dependence of electrical resistivity and relative heating power for SS316 tube

Consequently, the Center serves as the most reliable benchmark point for calibration. As evidenced by the resistivity analysis, the local heat flux at the Center aligns most closely with the axial average ($P_{local} \approx P_{avg}$), effectively neutralizing the systematic bias introduced by the DC heating system. Based on the median Amp95 over-prediction observed at this neutral location across all tested conditions, a representative correction factor of 252% was derived to establish a more realistic evaluation framework for advanced reactor designs.

4.2 Advanced Reactor HSG Thermal-Hydraulic Analysis

The modified MARS-KS code was utilized to evaluate the thermal-hydraulic behavior of the SMART and HTR-PM advanced reactor designs under their respective nominal operating conditions as shown in Table 6. The boundary conditions for each analysis were established based on the primary side heat source parameters and the secondary side helical tube inlet conditions. For the SMART analysis, the secondary side was modeled with an inlet pressure and temperature reflecting its system-integrated PWR characteristics, where the relatively lower operating pressure compared to the primary side enhances the sensitivity to phase-change boundaries. In contrast, the HTR-PM analysis was conducted under high-pressure and high-temperature conditions consistent with gas-cooled reactor specifications, resulting in a significantly reduced liquid-to-vapor density ratio.

Table VI: HSG Tube Side Boundary Condition in Advanced Reactor

Reactor	SMART	HTR-PM
Outlet pressure [MPa]	5.2	13.24
Mass flux [kg/m^2s]	472.7	1059
Feed water temperature [℃]	200	205
Main steam temperature [℃]	296	571
Length-inner diameter ratio	2083.3	4615.4
Structure material (Inconel)	690	800

In the HTR-PM cases, the two-phase region terminated relatively early because of the high primary-to-secondary temperature gradient, which created a long and stable superheated steam section. The stable density ratio ensured that the wall temperature amplitudes (Amp95) remained within a limited range as shown in figure 8. Conversely, the SMART conditions featured a boiling transition region located very close to the outlet, which caused the dryout point to fluctuate significantly in response to flow oscillations as shown in figure 9. Consequently, a progressive amplification of wall temperature oscillation amplitudes was observed toward the exit, demonstrating that the spatial distribution of thermal transients is highly dependent on the flow-regime distribution and the specific boundary conditions of the reactor design.

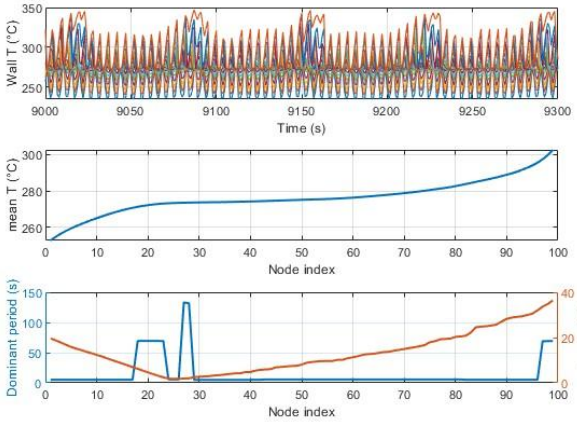

Fig. 8. SMART wall temperature behavior: (T) oscillations, (M) axial means, and (B) period/amplitude characteristics

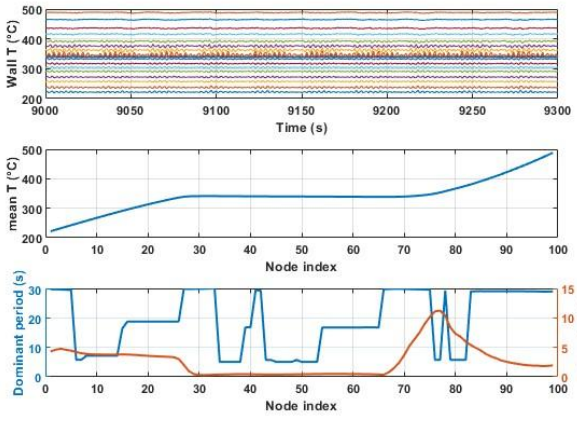

Fig. 9. HTR-PM wall temperature behavior: (T) oscillations, (M) axial means, and (B) period/amplitude characteristics

4.3 Evaluation of Thermal Fatigue Margins

The calculated thermal stress amplitudes ($\sigma_{corrected}$) followed a distribution trend consistent with the nodal temperature oscillation profiles (Amp95) obtained in Section 4.2. Analysis using various constraint factors(η) confirmed that while structural constraints alter the absolute stress levels, the peak stress locations are

primarily determined by the thermal-hydraulic characteristics dictated by the boundary conditions. To account for the quantified numerical conservatism of the code, the numerical stress results were adjusted using the derived correction factor. Specifically, since the MARS-KS code was found to over-predict the oscillation amplitude by a factor of 2.52 at the center, the raw numerical stress amplitudes ($\sigma_{numerical}$) were scaled down by dividing them by 2.52 as shown in Equation 4.

$$\sigma_{corrected} = \frac{\sigma_{numerical}}{2.52} = \eta \cdot E \cdot \alpha \frac{\Delta T_{MARS-KS}}{2.52} \quad (4)$$

This calibration effectively adjusted the stress levels while preserving the axial distribution trends and identifying peak stress locations. The final corrected results for both reactor designs were generally found to be within a range lower than the 92 MPa fatigue limit for Inconel 800 as shown in figures 10 and 11. This suggests that the thermal stresses induced by DWO under the evaluated conditions do not reach critical thresholds for immediate structural failure, proving that the proposed correction framework effectively balances engineering conservatism with operational realism.

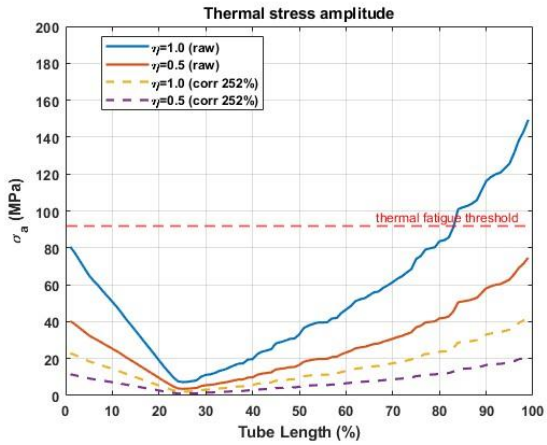

Fig. 10. Axial distribution of thermal stress under SMART conditions

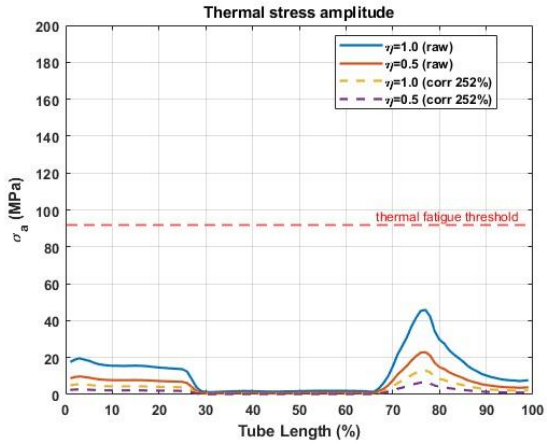

Fig. 11. Axial distribution of thermal stress under HTR-PM conditions

5. Conclusions

In this study, the thermal-hydraulic transients induced by Density Wave Oscillations (DWO) in helical steam generators (HSGs) were evaluated by validating the MARS-KS code with experimental data and performing a calibrated fatigue analysis for advanced reactor designs. The validation results demonstrated that while MARS-KS successfully captures the physical trend of decreasing oscillation periods with increasing pressure, it exhibits significant numerical conservatism by consistently over-predicting wall temperature amplitudes (Amp95) and frequency of fluctuations. These discrepancies are suggested to stem from fundamental property differences between the simulant fluid (Novec-649) and water-based correlations, as well as the systematic bias introduced by the non-uniform heat flux distribution in the experimental DC heating system. As a quick remedy to the situation, a correction framework was established using a 252% correction factor derived from the center.

The calibrated analysis for the HTR-PM and SMART reactor designs revealed distinct thermal-hydraulic responses dictated by their specific boundary conditions. The HTR-PM design exhibited stable behavior with limited temperature amplitudes due to high-pressure operation and an early transition to the superheated steam region. In contrast, the SMART design showed a progressive amplification of wall temperature fluctuation amplitudes toward the outlet under unstable conditions, where the boiling transition region was located.

Nevertheless, the evaluation of thermal fatigue margins confirmed that the corrected stress levels for both designs are generally within the 92 MPa fatigue limit for Inconel 800. This means that fatigue issue with DWO instability in HSG is less substantial then initially hypothesized. Notably, the comparative analysis of structural materials indicated that Inconel 800, utilized in the HTR-PM, is more susceptible to thermal stress compared to the Inconel 690 used in the SMART design, primarily due to its higher coefficient of thermal expansion and lower thermal conductivity. To enhance the fidelity of the current findings, future research should prioritize comparing predictions from system analysis codes with actual water-based experimental data to address the property differences of simulant fluids. A systematic evaluation of numerical factors, such as nodalization sensitivity and interfacial correlations, is also required to identify the key determinants of oscillation amplitudes in thermal-hydraulic systems.

ACKNOWLEDGEMENT

This work was supported by the National Research Fou ndation of Korea(NRF) grant funded by the Korea gove rnment (MSIT)(No. : RS-2024-00436693).

REFERENCES

[1] Z. Zhang, Z. Wu, D. Wang, F. Xu, Y. Sun, and F. Li, Current status and technical description of Chinese 2 × 250 MWth HTR-PM demonstration plant, Nuclear Engineering and Design, Vol. 239, p. 1212, 2009.
[2] J. Wang, L. Lin, H. Fu, and others, Evaluation of thermal fatigue life and crack morphology in brake discs of low-alloy steel for high speed trains, Engineering Failure Analysis, Vol. 35, p. 55, 2013.
[3] S. Oh, D. H. Kim, and J. I. Lee, Prediction of density wave oscillation in helical steam generators using the MARS-KS Code, International Journal of Heat and Mass Transfer, Vol. 235, 2024
[4] S. Oh, J. H. Hwang, D. H. Kim, T. Min, and J. I. Lee, Investigations of density wave oscillation in helical tubes with different configurations sharing the same inlet and outlet headers, Nuclear Engineering and Technology, Vol. 57, 2025.
[5] H. Ito, Friction Factors for Turbulent Flow in Curved Pipes, Journal of Basic Engineering, Vol. 81, p. 123, 1959.
[6] M. Colombo, L. P. M. Colombo, A. Cammi, and M. E. Ricotti, A scheme of correlation for frictional pressure drop in steam-water two-phase flow in helicoidal tubes, Chemical Engineering Science, Vol. 123, p. 460, 2015..